Advances in Nano Research, *Vol. 6 No. 4 (2018) 357-375*
DOI: https://doi.org/10.12989/anr.2018.6.4.357

Molecular interactions between pre-formed metal nanoparticles and graphene families

Serena Low [a] and Young-Seok Shon[*]

Department of Chemistry and Biochemistry, California State University, Long Beach, 1250 Bellflower Blvd., Long Beach, CA 90840, USA

(*Received December 16, 2017, Revised September 15, 2018, Accepted December 18, 2018*)

Abstract. Two dimensional (2D) atomic layered nanomaterials exhibit some of the most striking phenomena in modern materials research and hold promise for a wide range of applications including energy and biomedical technologies. Graphene has received much attention for having extremely high surface area to mass ratio and excellent electric conductivity. Graphene has also been shown to maximize the activity of surface-assembled metal nanoparticle catalysts due to its unique characteristics of enhancing mass transport of reactants to catalysts. This paper specifically investigates the strategy of pre-formed nanoparticle self-assembly used for the formation of various metal nanoparticles supported on graphene families such as graphene, graphene oxide, and reduced graphene oxide and aims at understanding the interactions between ligand-capped metal nanoparticles and 2D nanomaterials. By varying the functional groups on the ligands between alkyl, aromatic, amine, and alcohol groups, different interactions such as van der Waals, π-π stacking, dipole-dipole, and hydrogen bonding are formed as the 2D hybrids produced.

Keywords: nano-carbon; nanoparticle; nano-composites; nano-structures; nano-materials

1. Introduction

Two dimensional (2D) materials have the potential to revolutionize our energy, electronic, and biomedical technologies (Ferrari *et al*. 2015, Chen *et al*. 2015). The desire to produce sustainable energy and improve our current energy storage capabilities is prevalent (Ferrari *et al*. 2015, Liu *et al*. 2014). For example, we constantly seek electronic devices made of lighter-weight materials with longer-lasting batteries (Chmiola *et al*. 2010). Biologically compatible 2D materials that give rise to new platforms for targeted drug delivery and hyperthermia treatments toward tumor cells are also being developed (Yin *et al*. 2015).

Popular 2D atomic layered materials include graphene and its derivatives, transition metal dichalcogenides (TMDs), and transition metal oxides (TMOs) (Ferrari *et al*. 2015). The exfoliation of graphite to form graphene was discovered in 2004 and since then the study of its isolation and characterization has evolved into a vast area of chemistry with many major applications (Bhimanapati *et al*. 2015). Due to its highly crystalline structure and aromatic sp^2 carbon network, graphene has exceptional strength up to 48,000 $kN \cdot m \cdot kg^{-1}$ and allows for ultrahigh charge carrier

*Corresponding author, Ph.D., Professor, E-mail: ys.shon@csulb.edu
[a] Graduate Student

 ISSN: 2287-237X (Print), 2287-2388 (Online)

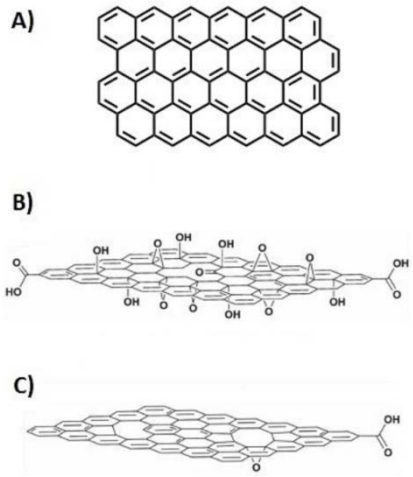

Fig. 1 Chemical structures of (A) graphene, (B) graphene oxide, and (C) reduced graphene oxide (Compton and Nguyen 2010]

mobility at just room temperature (Ferrari *et al*. 2015). Graphene has both excellent electronic capabilities and unmatched thermal conductivity up to 5000 $W \cdot m^{-1} \cdot K^{-1}$ (Yin *et al*. 2015). The 2D single atom-thick layered structures demonstrate a good surface area to mass ratio allowing for very flexible and lighter weight electronic materials. The transparency and flexibility of graphene would, therefore, allow for useful surface active applications in displays and touch screens.

The structural versatility of graphene is important for a broad range of applications. Graphene production ranges from nanoflakes to large near-meter scale rolls (Ferrari *et al*. 2015). Biomedical applications can utilize nano-graphene sheets due to the ease in cell-uptake (Chen *et al*. 2015, Yin *et al*. 2015). The surface of nano-graphene can be additionally functionalized by small organic or biological molecules for various applications such as drug delivery. The most popular derivatives of graphene are graphene oxide (GO) and reduced graphene oxide (rGO). A comparison of the chemical structures of graphene and its derivatives can be seen in Fig. 1 (Compton and Nguyen 2010).

The oxidation of graphene to GO leads to the formation of hydroxyl, epoxide, and carboxylic groups, the latter which protrude above and below the basal plane (Yin *et al*. 2015). Reduction strategies have been explored to partially restore the surface and electronic properties of GO to form rGO. The requisite value of graphene's quality and crystallinity is dependent on the desired application. The pristine sp^2 network of graphene provides an excellent platform for use in electronic devices. When functionalization of the surface is required, molecular noncovalent interactions rather than covalent bond formation are often preferred. It is because they do not modify the hybridization of graphene and preserve the aromaticity. Graphene and rGO are hydrophobic and are not directly compatible with biological systems. For biological applications, the hydrophilic and relatively less toxic GO is more popularly used (Yin *et al*. 2015).

Graphene materials combined with molecules or metal nanoparticles are of great interests due to the synergistic properties that lead to undiscovered applications (Ferrari *et al*. 2015, Chen *et al*. 2015). Currently, popular hybrid materials are formed by depositing noble metal nanoparticles onto the surface of graphene related materials. The 2D graphene-based substrate can act as a support structure for metal nanoparticles and reduce the nanoparticle aggregation, and can

ultimately enhance the catalytic activity by electronically or chemically facilitating reactions (Muszynski *et al*. 2008). Functionalizing the surface of these basic substrates with various polymers, organic, or biological molecules containing ionic or hydrophobic groups allow researchers to induce their desired surface interaction with ligand-capped metal nanoparticles. The strength of the bond between substrate and ligand of the metal nanoparticle can be studied by examining the functional groups on the substrates and ligands used. Herein, we investigate and compare the interactions of unfunctionalized and functionalized graphene materials with ligand-stabilized or ligand-free metal nanoparticles. The interactions discussed herein include polar-polar interaction via electrostatic force, nonpolar-nonpolar interaction via van der Waals force, aromatic-aromatic interaction via π-π stacking and lastly, covalent interaction (Yin *et al*. 2015). By understanding the synthetic methods to grow this relatively new class of graphene-based hybrid materials, one can optimize these materials for the desired applications and discover new applications created by the hybrid structures. For example, Zhu and associates functionalized the surface of graphene with an imidazolium salt-based ionic liquid (IS-IL) and electrostatically formed hybrids using citrated-stabilized Pt nanoparticles with potential applications of enhanced electrocatalysis to reduce oxygen (Zhu *et al*. 2009). Graphene has also been shown to enhance the efficiency of many photocatalysts with the intention to convert solar energy into chemical energy by converting water to hydrogen gas. The effect of graphene on TiO_2 nanoparticles as a hybrid photocatalyst has been explored by Xiang and Yu (2013). Well-designed and constructed graphene-related hybrid materials might enable new technologies and applications with radical advances.

2. Building blocks for nanocomposite materials

Two types of synthetic methods are used to form these nanoparticle hybrid materials. The ex-situ method requires metal nanoparticles to be pre-formed before they are introduced to the substrate material. The in-situ method involves the growth of metal nanoparticles directly onto the substrate. This latter route has often times shown the formation of polydispersed particles of varying shapes albeit the advance in improved synthesis of monodispersed or uniquely shaped nanoparticle has been recently reported (Bhaskar *et al*. 2017). The pre-formed nanoparticle method allows for better control of the size, shape and density (morphology) because monodispersed nanoparticles can be easily prepared in colloidal conditions using well established methods. By using pre-formed nanoparticles, we can make a more uniform hybrid material with consistent properties throughout. In addition, the pre-formed method eliminates any possible incompatibility that may develop when nanoparticles are grown onto the 2D surface.

Herein, we direct our efforts on hybrid materials made with pre-formed nanoparticles and 2D graphene derivatives in liquid phase. By looking at the factors that contribute to the formation of these materials, we can gain more systematic understandings on the effects of the components that enable the successful preparation of hybrid systems. The key components for hybrid synthesis in liquid phase are metal nanoparticles, ligand stabilizers (linkers), 2D substrates, and solvent system.

2.1 Metal nanoparticles

Noble metal nanoparticles have generated much interest due to their unique electronic, optical, catalytic, and photoresponsive properties (Yin *et al*. 2015). Spherical particles and nanorods are currently the most common shapes of metal nanoparticles though triangle, bipyramid, cube, and

dog bone-shaped nanoparticles have also been synthesized (Pan *et al*. 2015, Zhao *et al*. 2013, Zedan *et al*. 2013). Metal nanoparticles of Au, Ag, Cu, Pt, Pd, Ni, Ir, and bimetallic nanoparticles have been successfully synthesized using different synthetic methods (Gavia *et al*. 2015, Yin *et al*. 2015). Among these different metal nanoparticles, gold nanoparticles are frequently utilized in biological applications, because they are chemically inert to the body while optically active.

Two types of solution-phase synthetic methods are popularly used to prepare metal nanoparticles: ligand passivation process or seeding growth method (Zhao *et al*. 2013). The former method involves the reduction of metal precursors in the presence of capping ligands, which passivate the excessive nucleation-growth of particles to remain in nanoscale. The morphology and size of these nanoparticles can be precisely controlled by using different concentrations and types of reagents during their synthesis. This is the reason that the former method has been shown to provide a more monodispersed sample. The latter method involves small seed nanoparticles as the nucleation centers for growing into larger nanoparticles often with different shapes. The latter method is especially useful for the preparation of shaped nanoparticles with interesting optical and photoresponsive properties. The purity of starting materials and the synthesis condition used in the latter process have been found to have significant effects on the size and shape of nanoparticles.

2.2 Ligand stabilizers

Most metal nanoparticles are subject to irreversible aggregation and sometimes oxidation. Hence the stabilization of metal nanoparticles against these problems has been a prerequisite for direct applications of these structures in various technological applications. Various organic ligands with high metal surface affinity including thiol, sulfide, disulfide, thiosulfate, thioacetate, xanthate, phosphine, phosphine oxide, amine, ammonium complex, carboxylate, selenide, and isocyanide are used to improve the stability and reduce the aggregation of metal nanoparticles (Shon 2004, Zhao *et al*. 2013). The most common organic ligands used for physiological applications requiring aqueous environments and high salt concentrations are glutathione (GSH), citrate, and cetyltrimethylammonium bromine (CTAB). These ligands are self-assembled onto the surface of metal nanoparticles through electrostatic interactions or chemical bond formation and stabilize metal nanoparticles from aggregation and coarsening. The type of ligands chosen would control the chemical properties of nanoparticles including the solubility and the affinity to other materials or molecules.

2.3 2D atomic layered materials

Common synthetic techniques to make the 2D substrates include chemical vapor deposition (CVD) and wet chemical syntheses. The most commonly used 2D atomic layered substrates are graphene and its derivatives, graphene oxide (GO), and reduced graphene oxide (rGO). Because of its wide range of uses, GO suspended in water can now be commercially purchased. Reduced graphene oxide can be easily synthesized by the modified Hummers' method through the process of oxidizing graphite oxide followed by reducing oxygen functionalities (Ferrari *et al*. 2015, Yin *et al*. 2015). These graphene related materials have various functional groups exposed on their surfaces which enable the substrates to engage in different interactions with ligand-capped metal nanoparticles. The exposed functional groups of GO are carboxylic acid, alcohol, and epoxide while rGO primarily has alcohols on its surface. All types of graphene related materials maintain different levels of aromaticity.

2.4 Solvent and support systems

Depending on the type of solvent system used, two different assembly methods are most widely recognized: induced assembly and self-assembly. Water has been most beneficial to the use of hybrids for biological applications while organic solvents are often needed for device fabrication and catalysis. Due to the high dispersity of graphene materials in water and/or other organic solvents, polar solvents including THF and ethanol and nonpolar solvents such as hexane are used as medium for hybrid formations. Ideally, the metal nanoparticles or 2D supports are fully dissolved or dispersed in their respective solvents, preferably in the same solvent, prior to being mixed. This solvent system would allow for thermodynamic reorganization resulting in the most stable structure with lowest energy. The heterogeneous self-assembly of soluble metal nanoparticles on 2D substrates supported onto other insoluble solid materials is also a popular approach to generate the hybrids of metal nanoparticles and 2D supports. Induced assembly involves the metal nanoparticle and 2D substrate being in two different solvents before being combined together. Depending on how large of a polarity difference there is between the two solvents, the nanoparticles may have an aversion to one solvent that results in the attraction of the nanoparticle to the substrate.

3. Types of molecular interactions

Table 1 shown below reviews the current building blocks and successful preparation methods that are being used to assemble nanoparticle-2D hybrid materials in liquid phase. The molecular interactions or covalent bonds that form between ligand-capped metal nanoparticles and graphene-related substrates are investigated in order to understand designing concepts for stable and functional hybrid materials (Fig. 2). The following types of molecular interactions are the focus of our discussion: polar-polar interaction via electrostatic force, nonpolar-nonpolar interaction via van der Waals force, and aromatic-aromatic interaction via π-π stacking. The successful formations of stable hybrid materials based on covalent bonding or hydrogen bonding between two materials, albeit limited, are also presented. The lack of system using covalent bond formation might be due to the colloidal instability of either intermediates or hybrids generated during or after covalent bond forming reactions. Weaker interactions between nanoparticles and 2D substrates provide the equilibrium between hybrids and detached materials that might be required for maintaining high colloidal stability in liquid phase. Some specific examples are discussed in more detail in the following sections.

3.1 Polar-polar interaction via electrostatic force

Table 1 indicates that the self-assembly of metal nanoparticles by using electrostatic interactions between surface ligands and 2D supports is the most popular approach for building hybrid systems. For example, Chen and associates synthesized amine-functionalized CdS nanospheres (CdS NSPs) on rGO hybrid nanocomposites (CdS NSPs/GR) as effective photocatalysts for the selective reduction of nitro organics in the visible light region (Chen *et al*. 2013). Prior to the reduction of GO to rGO, the CdS NSPs were deposited onto the surface of GO. Aqueous GO solution was added to the as-prepared (3-aminopropyl)triethoxysilane (APTES)-modified CdS NSPs dispersion in ethanol at GO:CdS NPSs weight ratios of 0.02:1, 0.05:1, and 0.1:1 under vigorous stirring. The pH of the mixture was held at 6 and allowed to mix for 30 min.

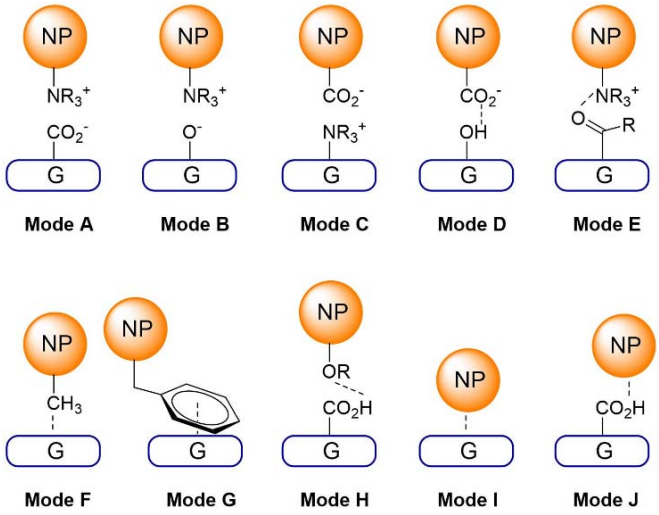

Fig. 2 Various molecular interactions used for the assembly of metal nanoparticles on graphene materials (NP: nanoparticle; G: graphene material; R: alkyl group

The final nanocomposites were collected by centrifugation and washed with deionized water. In this pH range, the GO colloids were stabilized by their own electrostatic repulsions. The positively charged amine groups on APTES were able to electrostatically self-assemble to the negatively charged deprotonated carboxyl groups ($-COO^-$) on GO.

The same strategy was used by Gupta and Subramanian, who synthesized rGO encapsulated $Bi_2Ti_2O_7$ (BTO) hybrid nanostructures in order to enhance the photocatalytic activity of band-gap engineered composite oxide nanostructures (BECON), bismuth titanate (Gupta and Subramanian 2014). Typically, BECONs experience problematic charge recombination on their surface. The introduced rGO acts as a charge separator between the oxide structures. Prior to the reduction of GO to rGO, 3-aminopropyltrimethoxysilane (APTMS)-functionalized BTO NPs dispersed in water were mixed with GO to form GBTO nanostructures. Acetic acid was added to the solution to achieve a pH ~3 and positively charge the surface of the NPs. Aqueous olutions of GO and ammonium hydroxide were mixed to achieve a pH ~8, which allows for the deprotonation of carboxylate groups and exposes negative charges on the surface of GO. The GO and BTO NPs solutions were mixed together by different BTO:GO weight ratios (1:0.0025, 1:0.0075, 1:0.01, and 1:0.06). The aqueous media allowed for the rapid self-assembly between positive and negative surface charges of the two materials. Zhou *et al*. (2013) prepared ternary nanocomposites based on the rGO-AuNP as a water-dispersive selective electrochemical sensing platform. By functionalizing both the rGO and AuNPs, Zhou *et al*. (2013) were able to design a hybrid material that enables the rGO to exhibit excellent recognition for select supramolecules and enhance the catalytic activity of AuNPs toward guest molecules. Citrate-capped AuNPs, about 3 nm in size, in water and amphiphilic pillar[5]arene-functionalized rGO (RGO-AP5) were mixed together with stirring and ultrasonication. The self-assembly of the AuNPs onto rGO in water is a result of the electrostatic interaction between the amino-group of AP5 on the surface of rGO and the citrate of AuNPs. The AP5 functionalization of the rGO surface is a result of both covalent and non-covalent bonding. A π-π interaction between the benzene rings of AP5 and the surface of rGO is another contributing interaction. Fig. 3 shows how the addition of AP5 aids in the dispersion of rGO in

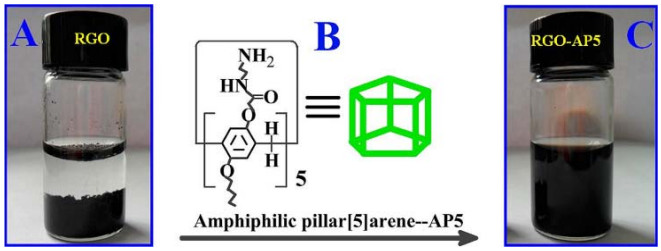

Fig. 3 (A) Photo of rGO in aqueous media; (B) Chemical structure of an amphiphilic pillar[5]arene [AP5]; (C) Photo of RGO-AP5 composites in aqueous media. (Zhou *et al*. 2013)

aqueous solution. The resulting rGO-AP5-AuNP hybrids were isolated from the solution by centrifugation.

Yao *et al*. (2013) developed a facile method for the self-assembly of citrate-stabilized gold nanoparticles onto N-(3-trimethoxysilylpropyl)diethylenetriamine-functionalized reduced graphene oxide (rGO-TSPD) in water. GO dispersed in ethanol was first functionalized by reacting with TSPD at 90°C. While the silane molecules covalently bond to the GO hydroxyl groups to form a silane monolayer, the amine groups of the organosilane aid in restoring the π bonds over the GO surface. At room temperature, pre-formed citrate-stabilized AuNP solution was mixed with rGO-TSPD solution. The exposed amine groups of the TSPD help to anchor the citrate-capped AuNPs onto the surface of GO by electrostatic forces. The deposited AuNPs were reported to have high density, good dispersity, and an average inter-particle distance of 15 nm. Figure 4 shows a schematic illustration of AuNP deposition onto rGO-TSPD (Left) and TEM images of the synthesized nanostructures (Right). These hybrid materials have the ability to sense single molecules like Rhodamine 6G (Rh6G) on its surface through surface-enhanced Raman spectroscopy (SERS).

Similarly, Zhu *et al*. (2009) reported the layer-by-layer (LBL) self-assembly of citrate-stabilized PtNPs onto 1-(3-aminopropyl)-3-methyl-imidazolium bromide-functionalized graphene sheets (G-IS-IL) to form three-dimensional hybrid nanostructures. The imidazolium salt-based ionic liquid (IS-IL) created positively charged ionic sites on the surface of graphene. This ionic liquid was reported as the "linker" between graphene and the negatively charged citrate-capped PtNPs. The average diameter of the PtNPs was confirmed to be 6 nm. After the 1-(3-aminopropyl)-3-methyl-imidazolium bromide linker was covalently bonded onto the graphene sheets, an indium-tin oxide (ITO) electrode was introduced to the solution for a 30-min initial coating process. Multilayer films were then created by alternately dipping the electrode into the PtNP solution and the G-IS-IL solution for 30 min each time. The electrostatic interaction between the IS-IL and citrate ligands allow the PtNPs to readily self-assemble onto the graphene sheets while in water. This new hybrid material has demonstrated high electrocatalytic activity for oxygen reduction. The electrocatalytic current and potential for this process can be easily adjusted by modifying the number of bilayers used to form these nanostructures. The LBL self-assembly process provides a novel method for the synthesis of hybrid electrochemical nanodevices. Similarly, Zhao *et al*. (2014) reported the fabrication of nanoscroll hybrid materials with the deposition of Fe_3O_4 NPs onto GO. This simple large-scale method to produce the nanoscroll structures has a great potential for high-performance energy storage in lithium-ion batteries. Two aqueous solutions of citrate-capped Fe_3O_4 and GO were directly combined together and sonicated for 5 min to allow for the full assembly of nanoparticles onto the GO.

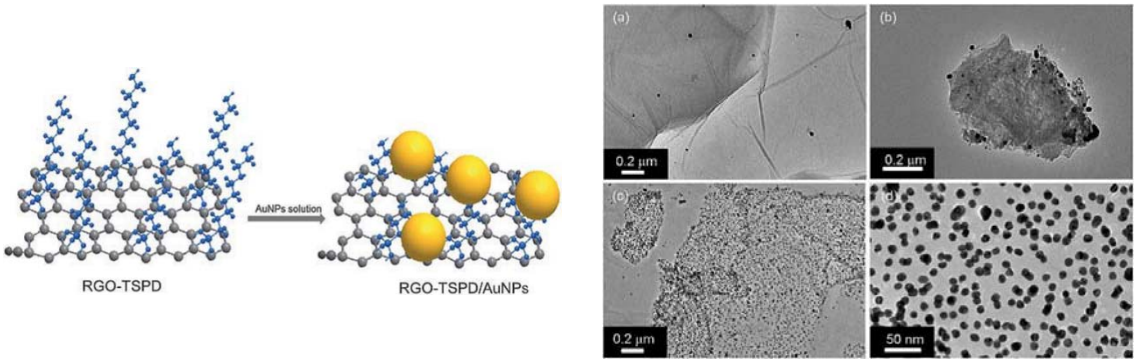

(A) (B)

Fig. 4 (A) Schematic illustration of AuNPs anchored on rGO-TSPD sheet through silane molecules (not drawn to scale): graphene sheet (grey), TSPD molecule (blue), AuNP (golden); (B) TEM images of (a) GO/AuNPs; (b) HRGO/AuNPs; and RGO-TSPD/AuNPs in (c) low magnification; and (d) high magnification. (Yao *et al*. 2013)

Zedan *et al*. (2013) were able to synthesize Au spherical nanoparticles and nanostructures of 7 varieties which included spheroids, short rods, long rods, bipyramids, rounded-corner rectangles, sharp-cornered rectangles, cubes, and dog bones. The AuNPs were citrate-stabilized while CTAB was used to cap the other nanostructures. To prepare the hybrid structure, AuNP or nanostructure solution was combined with GO solution. The hybrid materials were self-assembled via electrostatic interaction. The combined solution was irradiated in a quartz cuvette with a Nd:YAG laser of the second and third harmonics to further induce the assembly of AuNPs. Xu *et al*. (2013) synthesized GO-encapsulated AuNPs and NRs with a highly hydrophilic shell and low toxicity for biomedical applications. CTAB-stabilized AuNPs or NRs in water were combined with GO in water allowing for the electrostatic self-assembly of the Au particles onto the surface of GO. While the toxicity of CTAB was reduced when encapsulated by GO (GOe), the toxicity of GOe-AuNPs and GOe-AuNR hybrids was further reduced by the grafting of polyethylenimine (PEI) to the surfaces of GO. This PEI shell increases the hydrophilicity as well as the biocompatibility of the hybrid material.

Dembereldorj *et al*. (2014) prepared AuNR-GO nanocomposite materials for use as effective combination drug delivery platforms in photothermal cancer therapy. CTAB-stabilized AuNRs were pre-treated with HCl (10 M) until a pH of 1.4 was reached before the hybrid formation. 6-Arm polyethyleneglycol amine was used for PEGylation of the GO surfaces. To the PEG-functionalized GO solution, CTAB-capped AuNRs (55.2 ±1.1) dispersed in water were added. The treatment of AuNRs with HCl was used to reduce toxicity by removing some of the CTAB layers and the addition of PEG helped to increase the biocompatibility of GO. Ultimately, the AuNRs were encapsulated by PEG-GO and their cytotoxicity for *in vitro* and *in vivo* testing was further reduced. The amine group of PEG and positive charge on CTAB were able to interact electrostatically and enable the self-assembly of AuNR-PEG-GO in water. Hu *et al*. (2013) also synthesized AuNR-GO hybrid materials as effective SERS substrates for enhancing the signals of adsorbed aromatic cationic and anionic dye molecules using CTAB-stabilized AuNRs. To an aqueous dispersion of GO, poly(N-vinyl-2-pyrrolidone) (PVP) was added. This process was followed by the addition of aqueous CTAB-stabilized AuNRs. The hybrid materials were allowed to form by electrostatic self-assembly in water.

Table 1 Summary of various building blocks for nanocomposite materials

Ligand-stabilized metal nanoparticles	2D atomic layered substrates	Method of assembly	Notes / applications
APTES-functionalized CdS NPs in water APTES: (3-aminopropyl) triethoxysilane	GO in water	Electrostatic self-assembly - **Mode A**	Chen *et al*. (2013) - Wrapping or layering observed - Photocatalysis
APTMS-functionalized BTO NPs ($Bi_2Ti_2O_7$) in water (pH~3) APTMS: (3-aminopropyl) trimethoxysilane	rGO in water (pH~8)	Electrostatic self-assembly - **Mode B**	Gupta and Subramanian (2014) - Encapsulation of AuNRs by rGO observed - Photo and electrocatalysis
Citrate-capped AuNPs in water	AP5-functionalized rGO in water AP5: Amphiphilic pillar[5]arene	Electrostatic self-assembly - **Mode C**	Zhou *et al*. (2013) - Amino-group of AP5 to AuNP - Sensing
Citrate-stabilized AuNPs in water	TSPD-functionalized rGO in water TSPD: N^1-(3-trimethoxysilylpropyl) diethylenetriamine	Electrostatic self-assembly - **Mode C**	Yao *et al*. (2013) - SERS
Citrate-capped Pd NPs in water	rGO in water	H bonding self-assembly - **Mode D**	Huang *et al*. (2014) - Electrocatalysis
Citrate-stabilized Pt NPs in water	Imidazolium salt-based ionic liquid-functionalized graphene (G-IS-IL)	Electrostatic self-assembly - **Mode C**	Zhu *et al*. (2009) - Electrochemical device
Citrate-capped Fe_3O_4 NPs in water	GO in water	Electrostatic self-assembly - **Mode D**	Zhao *et al*. (2014) - Wrapping observed - Lithium ion battery
CTAB-stabilized AuNPs in water Citrate-capped AuNPs in water	GO in water	Electrostatic self-assembly - **Mode A** H bonding self-assembly - **Mode D**	Zedan *et al*. (2013) - 7 Different shaped particles used - Photothermal application
CTAB-stabilized AuNPs in water	GO in water	Electrostatic self-assembly - **Mode A**	Xu *et al*. (2013) - Encapsulation of AuNPs and NRs by GO observed - Gene therapy
CTAB-stabilized Au NR-PdNP core-shell structure	GO in water	Electrostatic self-assembly - **Mode A**	Tao *et al*. (2016) - Fuel cell

Table 1 Continued

Ligand-stabilized metal nanoparticles	2D atomic layered substrates	Method of assembly	Notes / applications
CTAB stabilized Au NRs (pH = 1.4, HCl-treated) in water	PEGylated GO (polyetheyleneglycol amine) in water	Electrostatic self-assembly - **Mode B**	Dembereldorj *et al*. (2014) - Encapsulation of AuNRs by GO observed - Photothermal cancer therapy
CTAB-stabilized Au NRs in water	PVP-stabilized GO in water PVP: Poly (N-vinyl-2-pyrrolidone)	Electrostatic self-assembly - **Mode E**	Hu *et al*. (2013) - SERS
CTAB-capped Au NRs in water	Graphene on silicon slide	Induced assembly VDW - **Mode F** Heterogeneous	Nguyen *et al*. (2014) - Drop-cast preparation - SERS
CTAB-capped Fe_3O_4 NP in water	Graphene foam in water	Electrostatic self-assembly - **Mode A**	Zhang *et al*. (2017) - Lithium ion battery
DMAP-stabilized AuNPs in water DMAP: (N,N-dimethylamino)pyridine	GO in water	Electrostatic self-assembly - **Mode B**	Choi *el al*. (2011) - Chemical catalysis
DMAP-stabilized AuNPs in water	GO and amine-functionalized GO in water	Electrostatic self-assembly - **Mode B**	Ahn *et al*. (2017) - Layer-by-layer GO-AuNP multilayer films - Electronic device
2-MPy-capped AuNPs in water MPy:	GO or rGO in water	π-π stacking self-assembly - **Mode G**	Huang *et al*. (2010) - SERS / Catalysis
Octylamine-stabilized $Ni_{30}Pd_{70}$ alloy NPs in hexane	Graphene in ethanol	Induced-assembly VDW - **Mode F** Heterogeneous	Göksu *et al*. (2014) - Chemical catalysis
Oleic acid and TOP-stabilized PbTe nanocrystals	Graphene on SiN	Induced assembly VDW - **Mode F** Heterogeneous	Robertson *et al*. (2014) - Drop-cast preparation - Optoelectronic device
Phenylethanethiol-stabilized Au_{25} NPs in THF	rGO in water	π-π stacking Induced assembly - **Mode G**	Ghosh *et al*. (2014) - Stability evaluation
Silica-coated Ag NPs in water	GO in water	H bonding self-assembly - **Mode H**	Salam *et al*. (2014) - Chemical catalysis
TOAB-coated AuNPs in toluene	Graphene film on electrode	VDW Self-assembly - **Mode F** Heterogeneous	Dalfovo *et al*. (2014) - SERS

Table 1 Continued

Ligand-stabilized metal nanoparticles	2D atomic layered substrates	Method of assembly	Notes / applications
Ligand-free metal oxide colloids (Pt, Pd, Au, Ag) in water	rGO in water with high pH	H bonding self-assembly - **Mode H**	Mondal and Jana (2014) (4 examples) - NPs stabilized by hydroxide - Electrocatalysis
Ligand-free Ag, Au, Pd NPs in water	Graphene	VDW Self-assembly - **Mode I** Heterogeneous	Granatier *et al*. (2012)
Ligand-free $Ni_{84}Pt_{16}$ NPs in hexane	Graphene in hexane	VDW Self-assembly - **Mode I**	Du *et al*. (2015) - Fuel cell
Ligand-free CuPd Alloy NPs in hexane	rGO in ethanol-hexane	Induced-assembly VDW - **Mode J**	Diyarbakir *et al*. (2015) - Chemical catalysis

Choi *et al*. (2011) reported the synthesis of AuNP-GO nanocomposites as highly efficient catalysts towards the reduction of nitroarenes. 4-Dimethylaminopyridine-stabilized AuNPs (DMAP-AuNPs) were mixed with GO in various AuNP:GO volume ratios (3:1, 1:1, 1:3, 1:5, and 1:15). The positive charge on DMAP attracts strongly to the negative charges on GO for good electrostatic assembly. There may also be π-π interactions between the aromatic pyridine of the DMAP ligand to conjugated domains on GO but this could not be confirmed.

3.2 Polar-polar interaction via H bonding

Huang *et al*. (2014) prepared hybrid structures of citrate-capped PdNPs on rGO with excellent catalytic activity and stability for ethanol oxidation and oxygen reduction reactions. As-synthesized rGO in water was combined with pre-formed citrate-capped PdNPs and ultrasonicated for 10 min. The PdNPs were reported to be about 3 nm in diameter and were monodispersed. Although this paper makes a case for the in-situ method, the final concentration of PdNPs produced and the proportions deposited to make the hybrid structures were not reported. With these parameters missing, the duplication of this process would be difficult. Salam *et al*. (2014) created AgNP-GO nanocomposite materials for use as an excellent coupling reaction catalyst that is highly stable, inexpensive, and with good recyclability. As-made silica-coated AgNPs were dissolved in water and the solution was added to actively stirring GO solution. Following an additional 15 min of stirring, hydrazine hydrate (98%, 1 mL) was added and the temperature was increased to 80°C. The final precipitate was washed with water before use in catalytic reactions. In this work, the AgNPs were pre-formed, but the reduction of GO occurred after the deposition of the particles onto its surface. The interaction between rGO and AgNPs with silica coating should be based on H bonding between oxygen moieties of two nanomaterials.

Mondal and Jana (2014) reported a surfactant-free method to synthesize noble metal-graphene nanocomposites (MGN) for use as high-performance fuel cell catalysts. These materials produce a strong current for the oxidation of ethanol and formic acid and exhibit good stability and recyclability. As-made partially reduced GO was redispersed in water by ultrasonication. Basic

colloidal metal oxide solutions (Pt, Pd, Au, and Ag) were prepared by the addition of varying amounts of NaOH. The resulting colloidal metal oxide/hydroxide solution was added to the rGO solution. A redox reaction occurred between the two colloids in solution that result in metal-metal oxide nanoparticles on the surface of partially reduced GO.

3.3 Nonpolar-nonpolar interaction via Van der Waals Force

Nguyen *et al*. (2014) fabricated high performance graphene-AuNR hybrid substrates for the detection of pesticides by SERS. The selected pesticides to be tested with these substrates were azinphos-methyl, carbaryl, and phosmet. The surface plasmon resonance of AuNRs could be easily adjusted to the laser excitation wavelength of Raman spectroscopy which makes them a favorable choice to be used on SERS substrates. The CTAB-capped AuNR solution was centrifuged down into a brown pellet and redispersed into aqueous solution. The AuNR solution was then drop-casted onto a monolayer graphene-coated silicon slide (G-AuNR). The slide was then sealed inside a Petri dish and incubated at 25°C until they were dried.

Robertson *et al*. (2014) created hybrid structures of PbTe nanocrystals on monolayer graphene for optoelectronics and semi-conductor materials. Oleic acid (OA) and trioctylphosphine (TOP)-terminated PbTe nanocrystals (30 mg/mL in toluene) were drop-casted onto SiN TEM grids coated with monolayer graphene. After the solvent was evaporated within 1-2 min, drops of hexane were used to wash away excess reactants. The resulting hybrid materials had a self-assembled monolayer superlattice. Ligand exchange was performed to remove the long chain ligands from NPs on graphene, which helped to reduce steric repulsion for closer contact between adjacent nanocrystals and the graphene substrate itself. Resulting aggregation was good for facile film formation and device application.

Ghosh *et al*. (2014) reported that phenylethanethiol-capped Au_{25} clusters ($Au_{25}(SCH_2CH_2Ph)_{18}$) can be used for cluster growth on the surface of rGO by solvent-induced assembly. As-synthesized Au_{25} clusters in THF was added to graphene in water with stirring. Uniform clusters of $Au_{135}(SCH_2CH_2Ph)_{57}^{+}$ were found on the surface of graphene after induced assembly indicating the size evolution of Au_{25} clusters upon contact with graphene. These clusters were in the mass range of the known stable cluster, $Au_{144}(SCH_2CH_2Ph)_{60}$. Göksu *et al*. (2014) synthesized graphene-supported NiPd alloy NPs (G-NiPd) as an efficient catalyst for tandem dehydrogenation of ammonia borane and hydrogenation of nitro/nitrile compounds. This catalyst is selective, reusable, and cost-effective. $Ni_{30}Pd_{70}$ alloy NPs were dispersed in hexane and mixed with graphene dispersed in ethanol. The mixture was sonicated for 2 h to allow for better deposition of NPs onto the surface of graphene. Göksu *et al*. (2014) report this process as solution phase self-assembly, though the combination of non-polar hexane and polar ethanol results in a solvent with mixed polarity causing induced-assembly for the NPs onto graphene.

Dalfovo *et al*. (2014) designed a platform of tetraoctylammonium bromide (TOAB)-coated AuNPs on graphene to measure electrical conductivity and the surface enhanced Raman scattering (SERS) activity of the biological dye Rhodamine B (RhB). Graphene film was produced by chemical vapor deposition (CVD) and transferred onto microfabricated interdigitated Au electrodes (IDA). Fig. 5 (Left) shows an example of an IDA where baseline electrical conductivity can be measured across the gold current collectors (Chmiola *et al*. 2010). In Dalfovo's work, a two-phase Brust-Schiffrin method was used to synthesize TOAB-functionalized AuNPs (4.39 ± 1.25 nm). A heterojunction was formed by immersing the graphene-coated IDA into a suspension of AuNPs in toluene through van der Waals self-assembly. This process was also performed with

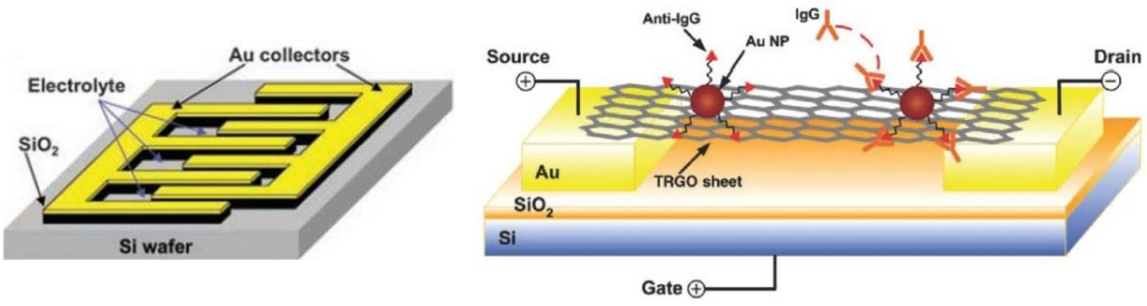

(A) (B)

Fig. 5 (A) An example of an interdigitated Au electrode (IDA) with gold current collectors integrated onto a silicon chip; (B) Protein detection using thermally reduced graphene oxide (TRGO) sheets decorated with gold nanoparticle—antibody conjugates. Anti-IgG is anchored to the TRGO sheet surface through AuNPs and functions as a specific recognition group for IgG binding. The electrical detection of protein binding is accomplished by FET and direct current measurements. (Chimiola *et al*. 2010)

GO film to produce a heterojunction sample for comparison. The polymer, poly(methyl methacrylate) (PMMA), is often used to prevent the oxidation of graphene grown through CVD. Unfortunately, PMMA is difficult to remove with conventional cleaning processes and remains as a residue on graphene compromising its electronic properties. Therefore, the conductivity of graphene was only measured to be 10^{-4} to 10^{-6} A. The graphene-AuNP heterojunction itself was discovered to quench photoluminescence and fluorescence while increasing SERS activity for RhB. In addition, Mao *et al*. (2010) reported the first graphene-AuNP hybrid sensor for the detection of immunoglobulin G (IgG) proteins.[38] This protein detector is constructed of anti-IgG antibodies that are covalently bonded to 20 nm AuNPs and anchored onto thermally reduced GO sheets (TRGO). When the target protein IgG is bound to the corresponding antibodies, detection is achieved through FET and direct current measurements. Fig. 5 (Right) is an illustration of this type of biosensor. The results of these studies can aid in the development of graphene field-effect transistors (G-FET) or SERS, and lead to the discovery of new biosensing devices.

Granatier *et al*. (2012) examined the interactions within surfactant-free noble metal nanoparticle-graphene composites through Möller–Plesset second-order perturbation theory (MP2) and density functional theory (DFT) calculations to understand their methods of binding. The hybrids were synthesized and then analyzed by SEM to qualitatively assess the noble metal NPs' affinity and interaction with the graphene sheets. Silver NPs were synthesized through reduction by D-maltose to an average particle size of 28 nm. Au and PdNPs were synthesized by using ascorbic acid as the reductant where 25 nm and 22 nm were the average core size, respectively. Graphene sheets were synthesized by CVD and then pre-formed noble metal nanoparticles of Pd, Au, and Ag in water were each mixed with separate aqueous colloidal graphene dispersions in a glovebox. Without any surfactant or ligands surrounding the noble metal NPs, they inherently possess nonpolar behavior. It is most likely that the NPs interact with the nonpolar surface of graphene via van der Waals force. Fig. 6 shows the SEM evaluation of each nanocomposite formed. Pd-graphene composites were uniformly covered by PdNPs without any agglomerates or free NPs unattached to the graphene. Conversely, for the Au-graphene and Ag-graphene hybrids, NPs and aggregates were observed to lie on and off of the graphene sheets. The aggregation indicates that the Au and AgNPs have a higher affinity to itself than the graphene, which was

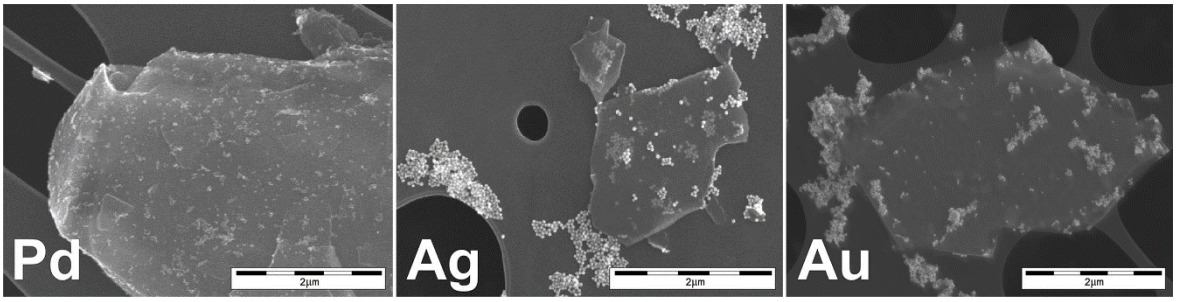

Fig. 6 SEM images of graphene−Pd (left), graphene−Ag (middle), and graphene−Au (right) composites (Granatier *et al*. 2012)

different from PdNPs. These results were consistent with the theoretical calculations performed.

Du *et al*. (2015) were able to prepare hybrid materials of NiPt NPs on graphene with high catalytic efficiency and good turnover frequency (TOF). As-synthesized, both ligand-free bimetallic NiPt NPs and graphene were dispersed in hexane and the solution was sonicated to allow for full interaction between the two components. This process was repeated with using NPs with varying compositions of Ni and Pt. $Ni_{84}Pt_{16}$/graphene had the highest catalytic activity with 100% selectivity for hydrogenation. Diyarbakir *et al*. (2015) also developed a process to deposit ligand-free CuPd nanoparticles onto rGO by self-assembly for use as hybrid catalysts in Sonogashira cross-coupling reactions. Reduced graphene oxide was dispersed in a mixed solvent system of ethanol/hexane (2:1). Bimetallic CuPd alloy nanoparticles dispersed in hexane were added to the rGO solution and the resulting mixture was then sonicated. The rGO-CuPd hybrid catalysts were precipitated out by the addition of ethanol, followed by centrifugation.

3.4 Nonpolar-nonpolar interaction via π-π stacking

Huang *et al*. (2010) synthesized 2-mercaptopyridine-capped Au nanoparticle-GO and –rGO nanocomposites through basic self-assembly in water. Modified Hummers' method was used to prepare GO and the reduction of GO resulted in rGO. Fig. 7 is a schematic illustration of the synthetic method used by Huang *et al*. (2010). Using Frens's method, 2-MPy-capped AuNPs were made and suspended in water until they were ready for use. Aqueous substrate solution containing either GO or rGO was combined with 2-MPy-capped AuNP solution. The resulting hybrid products were centrifuged for isolation and then washed with water. Huang *et al*. (2010) also noted that the hybrids were stable for 2 weeks. The aromatic 2-MPy ligands were able to strongly interact with the large delocalized sp^2 carbons on GO through π-π stacking. This physisorption process resulted in the anchoring of NPs onto the substrates. These Au-GO hybrid nanocomposites demonstrated exceptional SERS performance and with enhanced catalytic activity.

3.5 Covalent bond formation

Ismaili *et al*. (2011) synthesized rGO-AuNP hybrids using irradiated light to form covalent interactions between the two species. Reduced graphene oxide was dispersed in THF by sonication. 3-Aryl-3-(trifluoromethyl)diazirine-functionalized AuNPs (Diaz-AuNPs) in THF were combined with the rGO solution. The mixture was placed in a test tube, evacuated with argon for 15 min, and irradiated at wavelengths above 300 nm with a mercury lamp for 15 h while stirring. The

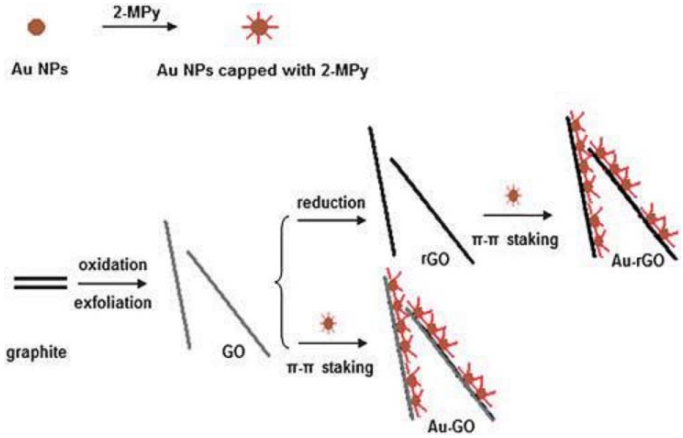

Fig. 7 Schematic illustration of the synthesis of Au-GO and Au-rGO composites. (Huang *et al*. 2010)

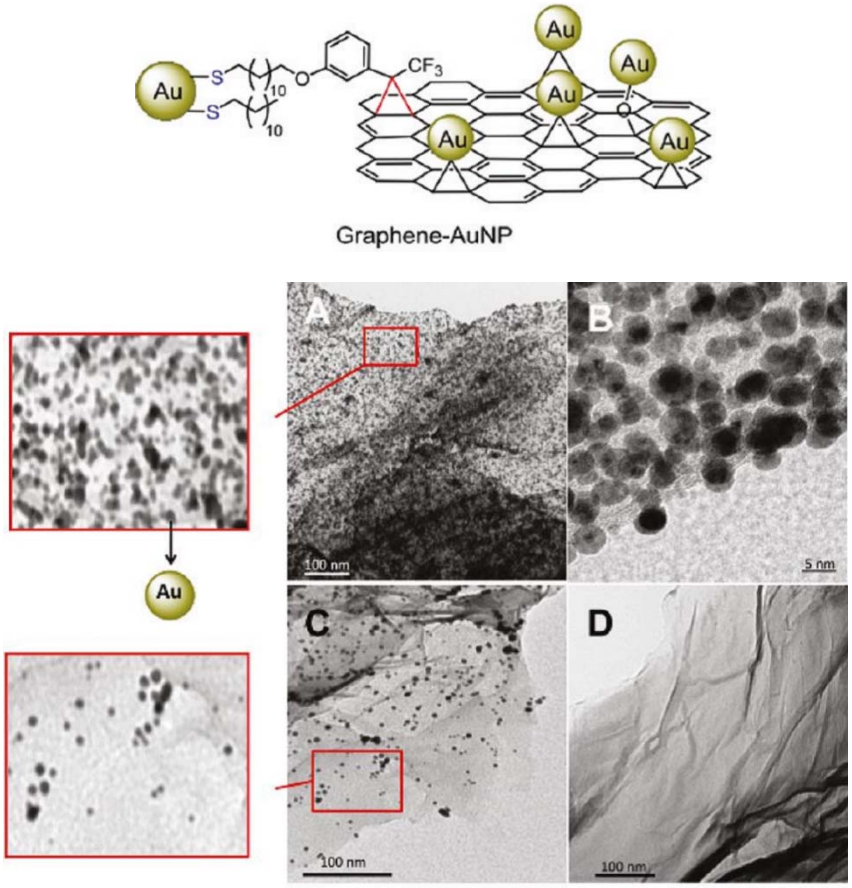

Fig. 8 Cartoon illustration of the carbene addition approach utilized for the covalent attachment of AuNPs onto graphene. (Top) TEM images of (A, B) graphene-AuNP hybrid after washing/purification protocol, (C) graphene after dark/control experiment (in the absence of UV irradiation and after the washing/purification protocol), and (D) unmodified graphene. (Bottom) (Ismaili *et al*. 2011)

irradiation induces the formation of covalent bonds between AuNPs and rGO. The diazirine moiety attached to the Diaz-AuNP turns to a carbene moiety upon irradiation at > 300 nm likely via secondary photolysis of a diazo-intermediate. The carbene functional groups can be either added to C = C bonds of graphene or accept the hydroxyl groups on the surface of GO or rGO. Fig. 8 (Top) illustrates the covalent bond formation of AuNPs to graphene through carbene addition. A control experiment was performed where the Diaz-AuNP/graphene mixture was stored in the dark and not irradiated. Only noncovalent interactions were present within the hybrid material. The weak interactions were confirmed by the removal of AuNPs after the standard washings used for the other samples. Fig. 8 shows a significantly lower population of AuNPs on graphene after the dark room experiment (Bottom, C) compared to where irradiation by light was used (Bottom, A).

4. Conclusions

A need to better control size, morphology, composition, density, and defects when synthesizing graphene-nanoparticle hybrids has been well recognized. This review focused on examining the assembly protocol for pre-formed ligand-capped gold nanoparticles onto 2D planar graphene substrates. Most 2D graphene-based metal nanocomposites developed and investigated for a variety of applications rely on the non-covalent interactions in the form of electrostatic force, van der Waals force, or hydrogen bonding as the main driving force for spontaneous nanoparticle assembly. Despite the extensive efforts to prepare nanoparticle-2D hybrid materials as shown in this review, the systematic studies regarding the stability of these hybrid materials are currently rather lacking in the literatures (Hrbek *et al*. 2008, Isaacs *et al*. 2006, Shon *et al*. 2011). The importance of structural integrity under the elevated temperature (Sugden *et al*. 2010) or light irradiation (Al-Sherbini 2010, Gordel *et al*. 2014) cannot be discounted due to the technological applications such as hyperthermia and catalysis applications (Horiguchi *et al*. 2008) that often require hostile conditions. For example, unfriendly physical conditions are often times necessary to activate the adsorbed pre-formed nanoparticles that are vulnerable to changes in size and shape when they are exposed to heat or light irradiation (Tan *et al*. 2013). In addition, since metal nanoparticles anchored on graphene families could exhibit interesting catalytic, electrical and optical activities (Bae *et al*. 2011, Hu *et al*. 2013), understanding the nature and extent of morphological transformation of nanoparticle-graphene hybrids under various conditions could maximize their potentials for many practical applications (Tan *et al*. 2013, Zhuo *et al*. 2013).

Direct comparison of thermal stability between gold nanoparticle-graphene oxide hybrids and free standing gold nanoparticles suggests that graphene oxide could facilitate rapid coarsening of gold cores (Pan *et al*. 2015). For gold nanorod-graphene oxide hybrids, graphene oxide would cause complete reshaping of gold nanorods during heat treatments at only 50°C by disrupting and stripping the protecting organic ligands from the surface of nanorods. The gradual changes in size and shape of nanoparticles, when they are exposed to heat or light irradiation could seriously impede their long-term technological advancements for device and catalysis applications. Therefore, further understanding of various factors determining morphological transformations of nanoparticles is required for developing new strategies for improving their overall stability and performance.

Acknowledgments

The research described in this paper was financially supported by the W.M. Keck Foundation and the National Institute of General Medical Science (GM089562).

References

Ahn, E., Lee, T., Gu, M., Park, M., Min, S.H. and Kim, B.-S. (2017), "Layer-by-layer assembly for graphene-based multilayer nanocomposites: the field manual", *Chem. Mater.*, **29**, 69-79.

Al-Sherbini, E.-S.A.M. (2010), "UV-visible light reshaping of gold nanorods", *Mater. Chem. Phys.*, **121**, 349-353.

Bae, H.S., Seo, E., Jang, S., Park, K.H. and Kim, B.-S. (2011), "Hybrid gold nanoparticle-reduced graphene oxide nanosheets as active catalysts for highly efficient reduction of nitroarenes", *J. Mater. Chem.*, **21**, 15431-15436.

Bhaskar, R., Joshi, H., Sharma, A.K. and Singh, A.K. (2017), "Reusable catalyst for transfer hydrogenation of aldehydes and ketones designed by anchoring palladium as nanoparticles on graphene oxide functionalized with selenated amine", *ACS Appl. Mater. Interf.*, **9**, 2223-2231.

Bhimanapati, G.R. *et al*. (2015), "Recent advances in two-dimensional materials beyond graphene", *ACS Nano*, **9**, 11509-11539.

Chen, Z., Liu, S., Yang, M.-Q. and Xu, Y.-J. (2013), "Synthesis of uniform CdS nanospheres/graphene hybrid nanocomposites and their application as visible light photocatalyst for selective reduction of nitro organics in water", *ACS Appl. Mater. Interf.*, **5**, 4309-4319.

Chen, Y., Tan, C., Zhang, H. and Wang, L. (2015), "Two-dimensional graphene analogues for biomedical applications", *Chem. Soc. Rev.*, **44**, 2681-2701.

Chmiola, J., Largeot, C., Taberna, P.-L., Simon, P. and Gogotsi, Y. (2010), "Monolithic carbide-derived carbon films for micro-supercapacitors", *Science*, **328**, 480-483.

Choi, Y., Bae, H.S., Seo, E., Jang, S., Park, K.H. and Kim, B.-S. (2011), "Hybrid gold nanoparticle-reduced graphene oxide nanosheets as active catalysts for highly efficient reduction of nitroarenes", *J. Mater. Chem.*, **21**, 15431-15436.

Compton, O.C. and Nguyen, S.T. (2010), "Graphene oxide, highly reduced graphene oxide, and graphene: versatile building blocks for carbon-based materials", *Small*, **6**, 711-723.

Dalfovo, M.C., Lacconi, G.I., Moreno, M., Yappert, M.C., Sumanasekera, G.U., Salvarezza, R.C. and Ibanez, F.J. (2014), "Synergy between graphene and Au nanoparticles (heterojunction) towards quenching, improving Raman signal, and UV light sensing", *ACS Appl. Mater. Interf.*, **6**, 6384-6391.

Dembereldorj, U., Choi, S.Y., Ganbold, E.-O., Song, N.W., Kim, D., Choo, J., Lee, S.Y., Kim, S. and Joo, S.-W. (2014), "Gold nanorod-assembled PEGylated graphene-oxide nanocomposites for photothermal cancer therapy", *Photochem. Photobiol. Sci.*, **90**, 659-666.

Diyarbakir, S., Can, H. and Metin, Ö. (2015), "Reduced graphene 0xide-supported CuPd alloy nanoparticles as efficient catalysts for the Sonogashira cross-coupling reactions", *ACS Appl. Mater. Interf.*, **7**, 3199-3206.

Du, Y., Su, J., Luo, W. and Cheng, G. (2015), "Graphene-supported nickel—platinum nanoparticles as efficient catalyst for hydrogen generation from hydrous hydrazine at room temperature", *ACS Appl. Mater. Interf.*, **7**, 1031-1034.

Ferrari, A.C., *et al*. (2015), "Science and technology roadmap for graphene, related two-dimensional crystals, and hybrid systems", *Nanoscale*, **7**, 4598-4810.

Gavia, D.J., Do, Y., Gu, J. and Shon, Y.-S. (2014), "Mechanistic insights into the formation of dodecanethiolate-stabilized magnetic iridium nanoparticles: thiosulfate vs thiol ligands", *J. Phys. Chem. C*, **118**, 14548-14554.

Ghosh, A., Pradeep, T. and Chakrabarti, J. (2014), "Coalescence of atomically precise clusters on graphenic

surfaces", *J. Phys. Chem. C*, **118**, 13959-13964.
Göksu, H., Ho, S.F., Metin, Ö., Korkmz, K., Garcia, A.M., Gultekin, M.S. and Sun, S. (2014), "Tandem dehydrogenation of ammonia borane and hydrogenation of nitro/nitrile compounds catalyzed by graphene-supported NiPd alloy nanoparticles", *ACS Catal.*, **4**, 1777-1782.
Gordel, M., Olesiak-Banska, J., Matczyszyn, K., Nogues, C., Buckle, M. and Samoc, M. (2014), "Post-synthesis reshaping of gold nanorods using a femtosecond laser", *Phys. Chem. Chem. Phys.*, **16**, 71-78.
Granatier, J., Lazar, P., Prucek, R., Šafářová, K., Zbořil, R., Otyepka, M. and Hobza, P. (2012), "Interaction of graphene and arenes with noble metals", *J. Phys. Chem. C*, **116**, 14151-14162.
Gupta, S. and Subramanian, V. (2014), "Encapsulating $Bi_2Ti_2O_7$ (BTO) with reduced graphene oxide (RGO): an effective strategy to enhance photocatalytic and photoelectrocatalytic activity of BTO", *ACS Appl. Mater. Interf.*, **6**, 18597-18608.
Horiguchi, Y., Honda, K., Kato, Y., Nakashima, N. and Niidome, Y. (2008), "Photothermal reshaping of gold nanorods depends on the passivating layers of the nanorod surfaces", *Langmuir*, **24**, 12026-12031.
Hrbek, J., Hoffmann, F.M., Park, J.B., Liu, P., Stacchiola, D., Hoo, Y.S., Ma, S., Nambu, A., Rodriguez, J.A. and White, M.G. (2008), "Adsorbate-driven morphological changes of a gold surface at low temperature", *J. Am. Chem. Soc.*, **130**, 17272-17273.
Hu, C., Rong, J., Cui, J., Yang, Y., Yang, L., Wang, Y. and Liu, Y. (2013), "Fabrication of a graphene oxide-gold nanorod hybrid material by electrostatic self-assembly for surface-enhanced Raman scattering", *Carbon*, **51**, 255-264.
Huang, J., Zhang. L., Chen, B., Ji, N., Chen, F., Zhang, Y. and Zhang, Z. (2010), "Nanocomposites of size-controlled gold nanoparticles and graphene oxide: formation and applications in SERS and catalysis", *Nanoscale*, **2**, 2733-2738.
Huang, Y.-X., Xie, J.-F., Zhang, X., Xiong, L. and Yu, H.-Q. (2014), "Reduced graphene oxide supported palladium nanoparticles via photoassisted citrate reduction for enhanced electrocatalytic activities", *ACS Appl. Mater. Interf.*, **6**, 15795-15801.
Isaacs, S.R., Choo, H., Ko, W.-B. and Shon, Y.-S. (2006), "Chemical, thermal, and ultrasonic stability of hybrid nanoparticles and nanoparticle multilayer films", *Chem. Mater.*, **18**, 107-114.
Ismaili, H., Geng, D., Sun, A.X., Kantzas, T.T. and Workentin, M.S. (2011), "Light-activated covalent formation of gold nanoparticle-graphene and gold nanoparticle-glass composites", *Langmuir*, **27**, 13261-13268.
Liu, M., Zhang, R. and Chen, W. (2014), "Graphene-supported nanoelectrocatalysts for fuel cells: synthesis, properties, and applications", *Chem. Rev.*, **114**, 5117-5160.
Mao, S., Lu, G., Yu, K., Bo, Z. and Chen, J. (2010), "Specific protein detection using thermally reduced graphene oxide sheet decorated with gold nanoparticle-antibody conjugates", *Adv. Mater.*, **22**, 3521-3526.
Mondal, A. and Jana, N.R. (2014), "Surfactant-free, stable noble metal—graphene nanocomposite as high performance electrocatalyst", *ACS Catal.*, **4**, 593-599.
Muszynski, R., Seger, B. and Kamat, P.V. (2008), "Decorating graphene sheets with gold nanoparticles", *J. Phys. Chem. C.*, **112**, 5263-5266.
Nguyen, T.H.D., Zhang, Z., Mustapha, A., Li, H. and Lin, M. (2014), "Use of graphene and gold nanorods as substrates for the detection of pesticides by surface enhanced Raman spectroscopy", *J. Agric. Food Chem.*, **62**, 10445-10451.
Pan, H., Low, S., Weerasuriya, N. and Shon, Y.-S. (2015), "Graphene Oxide-Promoted Reshaping and Coarsening of Gold Nanorods and Nanoparticles", *ACS Appl. Mater. Interf.*, **7**, 3406-3413.
Robertson, A.W., Ford, C., He, K., Kirkland, A.I., Watt, A.A.R. and Warner, J.H. (2014), "PbTe nanocrystal arrays on graphene and the structural influence of capping ligands", *Chem. Mater.*, **26**, 1567-1575.
Salam, N., Sinha, A., Roy, A.S., Mondal, P., Jana, N.R. and Islam, S.M. (2014), "Synthesis of silver—graphene nanocomposite and its catalytic application for the one-pot three-component coupling reaction and one-pot synthesis of 1,4-disubstituted 1,2,3-triazoles in water", *RSC Adv.*, **4**, 10001-10012.
Shon, Y.-S. (2004), "Metal nanoparticles protected with monolayers: synthetic methods", *Dekker Encyclopedia of Nanoscience and Nanotechnology*; (Schwarz J.A. Ed.), Marcel Dekker, New York, NY, USA, pp. 1-11.

Shon, Y.-S., Aquino, M., Pham, T.V., Rave, D., Ramirez, M., Lin, K., Vaccarello, P., Lopez, G., Gredig, T. and Kwon, C. (2011), "Stability and morphology of gold nanoisland arrays generated from layer-by-layer assembled nanoparticle multilayer films: effects of heating temperature and particle size", *J. Phys. Chem.* C, **115**, 10597-10605.

Sugden, M.W., Richardson, T.H. and Leggett, G. (2010), "Sub-10 Ω resistance gold films prepared by removal of ligands from thiol-stabilized 6 nm gold nanoparticles", *Langmuir*, **26**, 4331-4338.

Tan, C., Huang, X. and Zhang, H. (2013), "Synthesis and applications of graphene—based noble metal nanostructures", *Mater. Today*, **16**, 29-36.

Tao, Y., Dandapat, A., Chen, L., Huang, Y., Sasson, Y., Lin, Z., Zhang, J., Guo, L. and Chen, T. (2016), "Pd-on-Au supra-nanostructures decorated graphene oxide: an advanced electrocatalyst for fuel cell application", *Langmuir*, **32**, 8557-8564.

Xiang, Q. and Yu, J. (2013), "Graphene-based photocatalysts for hydrogen generation", *J. Phys. Chem. Lett.*, **4**, 753-759.

Xu, C., Yang, D., Mei, L., Lu, B., Chen, L., Li, Q., Zhu, H. and Wang, T. (2013), "Encapsulating gold nanoparticles or nanorods in graphene oxide shells as a novel gene vector", *ACS Appl. Mater. Interf.*, **5**, 2715-2724.

Yao, H., Jin, L., Sue, H-J., Sumi, Y. and Nishimura, R. (2013), "Facile decoration of Au nanoparticles on reduced graphene oxide surfaces via a one-step chemical functionalization approach", *J. Mater. Chem. A*, **1**, 10783-10789.

Yin, P.T., Shah, S., Chhowalla, M. and Lee, K.-B. (2015), "Design, synthesis, and characterization of graphene—nanoparticle hybrid materials for bioapplications", *Chem. Rev.*, **115**, 2483-2531.

Zedan, A.F., Moussa, S., Terner, J., Atkinson, G. and El-Shall, M.S. (2013), "Ultrasmall gold nanoparticles anchored to graphene and enhanced photothermal effects by laser irradiation of gold nanostructures in graphene oxide solutions", *ACS Nano*, **7**, 627-636.

Zhang, N., Yan, X., Huang, Y., Li, J., Ma, J. and Ng, D.H.L. (2017), "Electrostatically assembled magnetite nanoparticles/graphene foam as a binder-free anode for lithium ion battery", *Langmuir*, **33**, 8899-8905.

Zhao, P., Li, N. and Astruc, D. (2013), "State of the art in nanoparticle synthesis", *Coord. Chem. Rev.*, **257**, 638-665.

Zhao, J., Yang, B., Zheng, Z., Yang, J., Yang, Z., Zhang, P., Ren, W. and Yan, X. (2014), "Facile preparation of one-dimensional wrapping structure: graphene nanoscroll-wrapped of Fe_3O_4 nanoparticles and its application for lithium-ion battery", *ACS Appl. Mater. Interf.*, **6**, 9890-9896.

Zhou, J., Chen, M., Xie, J. and Diao, G. (2013), "Synergistically enhanced electrochemical response of host—guest recognition based on ternary nanocomposites: reduced graphene oxide-amphiphilic pillar[5]arene-gold nanoparticles", *ACS Appl. Mater. Interf.*, **5**, 11218-11224.

Zhu, C., Guo, S., Zhai, Y. and Dong, S. (2009), "Layer-by-layer self-assembly for constructing a graphene/platinum nanoparticle three-dimensional hybrid nanostructure using ionic liquid as a linker", *Langmuir*, **26**(10), 7614-7618.

Zhuo, Q., Ma, Y., Gao, J., Zhang, P., Xia, Y., Tian, Y., Sun, X., Zhong, J. and Sun, X. (2013), "Facile synthesis of graphene/metal nanoparticle composites via self-catalysis reduction at room temperature", *Inorg. Chem.*, **52**, 3141-3147.

CC